Case Studies in Thermal Engineering 50 (2023) 103431

Contents lists available at ScienceDirect

Case Studies in Thermal Engineering

journal homepage: www.elsevier.com/locate/csite

A novel experimental design for free energy from the heat-gaining panel using multi-thermoelectric generators (TEGs) panel

Hiba Ali Hussein [a], Zhonglai Wang [a,*], W.K. Alani [b,c], J. Zheng [b], M.A. Fayad [c]

[a] School of Mechanical and Electrical Engineering, University of Electronic Since and Technology of China, Chengdu, 610031, China
[b] Tribology Research Institute, Key Laboratory of Advanced Technologies of Materials, Ministry of Education, Southwest Jiaotong University, Chengdu, 610031, China
[c] Energy and Renewable Energies Technology Center, University of Technology- Iraq, Baghdad, Iraq

HIGHLIGHTS

- A novel experimental design for free energy has less effect on environment and energy consumption.
- Thermoelectric generators (TEGs) panel can generate a good amount of energy and cost.
- TEGs panel generates electric powers of 8.04437 W and 80.40171 W during the cubic ice and sunlight tests.
- The maximum electric power and a maximum efficiency were (η) 57.44 W and 19.3% respectively.
- The efficiency of TEGs panel is higher from ice test by 16.243% compared to the sun test by 10.277%.

ARTICLE INFO

Keywords:
Heat-gaining
Thermal power
Thermoelectric generators
TEGs panel
Semiconductors
Free energy

ABSTRACT

Thermoelectric generators (TEGs) panel is used to produce electrical energy by converting thermal energy into electrical energy depending on the temperature differences (ΔT) between the two sides of the panel, which can generate electrical power over 24 h for different climate conditions (hot, cold, wet or dry). The TEGs panel was designed using Solidworks and the prototype of the TEGs panel was carried out in this study for practical testing and evaluation. The TEGs panel performances and the limitation, including parameters such as power generation, efficiency, response time was studied. In this study, the TEGs panel was exposed to sunlight and cubic ice to consider temperature variations throughout the day. The results showed that the TEGs panel generates electric powers of 8.04437 W and 80.40171 W during the cubic ice and sunlight tests, respectively, for temperature differences (ΔT) of 18 °C and 3.3 °C. The electric power from this test can be used to charge a small mobile phone. It was indicated that the theoretical results by the MATLAB program are closely resemble the laboratory results. Furthermore, the correction ratio for the power of MATLAB validation was 6.59%, while the correction ratio for the efficiency was 5.46%. The response time of the system was ranged from 2 to 6 min, which it is indicating the time needed for the TEGs panel to respond effectively to changes in temperatures. After incorporating the correction ratios from MATLAB simulation, the results showed that the maximum electric power and a maximum efficiency (η) are 57.44 W and 13.5%, respectively, when the temperatures difference (ΔT) reaches 70 °C. This study presents a prototype of a versatile power generator (TEGs panel) offers free energy which can be utilising in insulation of building walls and power generation at the same time.

* Corresponding author.
E-mail address: wzhonglai@uestc.edu.cn (Z. Wang).

https://doi.org/10.1016/j.csite.2023.103431
Received 26 June 2023; Received in revised form 11 August 2023; Accepted 27 August 2023
Available online 1 September 2023

1. Introduction

Solar energy systems have limitations due to their dependence on sunlight availability and intermittent energy production. Fluctuations in energy generation can occurred throughout the day and it's influenced by weather conditions. To overcome these on obstacles, the researchers tried to find another sources of free energy such as energy storage systems, semiconductors pieces and thermal power. The idea of thermoelectric generators (TEGS) panel emerged because of a set of problems that people are currently experiencing. These problems are summarized in several aspects, the most important issue is energy which represent the general issue in the world, the cost of energy production, the negative impact on the environment, and renewable energy technologies that currently used. Recently, it should also note that the high consumption of electric power by the consumer causes an increasing burden on governments or companies producing energy with the growing population in various parts of the world. It is reported that the TEGs panel used the heat produced by the combustion of natural gas, butane or propane [1]. The burner heats one side of the lead-tin-telluride TE modules directly, while the other side of the modules equipped with fins is cooled by natural convection. Furthermore, the TEGs systems are used on gas pipelines, wellheads, offshore platforms, telecommunications sites, and security surveillance. Previous study presented the development and characterization of a thermoelectric generator (TEG) system for waste heat recovery to low temperature in industrial processes. The characterization of TEGs that are used a data-acquisition system have measured data for the voltage, current, and temperature, in real-time, for temperatures down to 200 °C without signal degradation. As a result, the measured data has revealed an open circuit voltage of $VOC = 0.4306 \times \Delta T$, internal resistance of $R0 = 9.41\ \Omega$, with tolerance $\Delta Rint = \pm 0.77\ \Omega$, where $Rint = 9.41 \pm 0.77\ \Omega$. The measurements were made on the condition that the maximum output was obtained at a temperature gradient of $\Delta T = 80\ ^\circ C$, resulting in a maximum power gain of Pout ≈29 W. X.F. Zheng et al. [2] integrated the thermoelectric cogeneration to the existing domestic boiler using a thermal cycle and enable the system to utilise the unconverted heat, which represents over 95% of the total absorbed heat, to preheat feed water for domestic boiler. The experimental study, based on a model scale prototype which consists of oriented designs of heat exchangers and system construction configurations. An introduction to the design and performance of heat exchangers has been given. A theoretical modeling for analyzing the system performance has been established for a good understanding of the system performance at both the practical and theoretical level. Insight has also been shed onto the measurements of the parameters that characterize the system performance under steady heat input. The system performance including electric performance, thermal energy performance, hydraulic performance and dynamic thermal response are introduced [3]. Seepana PraveenKumar et al. [4] presented a thermo-enviro-economic analysis for a hybrid photovoltaic (PVT)/thermoelectric generator (TEGs) system. A comparative investigation between a reference PV, PVT with water, and PVT with TEG/nanofluid was performed. The key findings from the comparative study revealed that the compared to the reference PV panel, the temperature drop of the PVT/Water, and PVT/TEG/nanofluid configurations are found to be 25.1%, and 41.2%, respectively. The electrical efficiencies of the PVT/Water, and PVT/TEG/nanofluid panels also improved by 5.8%, and 8.5%, respectively. Furthermore, it was found that the levelized cost of energy (LCOE), energy payback time (EPBT), and the environmental impact (net CO2 mitigation, and carbon credit) achieved for the PVT/TEG/nanofluid system, are 0.051–0.178 $/kWh, 3.36 years, 2.07 ton/year, 51.94 $/year, respectively. The LCOE and EPBT were found to be relatively high for the PVT/TEG/nanofluid system, compared to that of the PVT/Water, and reference PV module due to the extra cost incurred in its construction materials. Mohammed A. Qasim et al. [5] designed a Maximum Power Point Tracking (MPPT) technique for a TEG module. The module is built using 204 TEGs connected in series. It is connected to the load through a DC/DC boost converter. The MPPT technique used in this work is the Interval Type 2 Fuzzy Logic Controller (IT2FLC). To verify its performance, the IT2FLC is compared with a traditional Perturb and Observe (P&O) MPPT algorithm in the case of power and voltage response at steady state, load switching, and through various ranges of temperature differences (DT). The TEG module is modeled and the whole system is simulated successfully using MATLAB SIMULINK R2017a. Previous study by Zheng et al. [6] presented a complex domestic system combining a gas boiler and a solar concentrator with two TEG blocks. The domestic hot water is preheated on the cold side of the TEG units. The heat is provided either by the hot gas of the boiler or by the hot oil of the TEG. The experiments have mainly been conducted on oil-powered TEGs. Kraemer et al. [7] and McEnaney et al. [8] have demonstrated a flat-panel solar thermal-to-electric power conversion technology. The concentrating solar thermoelectric generators (STEGs) consist of an optical concentration system and thermal concentration absorber. A glass enclosure envelops the absorber and the TEG to maintain a vacuum as well as reduce thermal losses. The developed STEGs achieved a peak efficiency of 4.6% under 1 kW m^2 solar conditions. The difficulty for this kind of generator is concentrating the heat on the thermoelectric elements and finding materials that can withstand very high temperatures (>1000 C).

It is studied a double-pass TE solar air collector with flat plate reflectors [9]. The flat plate reflectors were used to concentrate solar radiation onto the TE solar air collector. In addition, the optimum position of the reflectors was studied and they produced 2.1 W of the power. The works by He et al. [10,11] investigated the coupling of solar water heating with a TEG. The experimental results from the above studies were based on a solar concentrator with glass-evacuated tubes. The heat pipe transfers the solar heat absorbed within the glass-evacuated tube to a water channel. The TEG works as a heat exchanger between the heat pipe and the water channel. The electrical efficiency was low at around 1–2%, while the overall efficiency must be taken into account in solar heat pipe TEG (SHP-TEG) system. The efficiency of hot water production is quite good about 55%. A solar hybrid electric/thermal system with a radiation concentrator was presented by two works of Chavez-Urbiola et al. [12,13]. The system generates 20 W of electrical energy and 200 W of thermal energy stored in water at around 50 °C. The performance of this combined solar photovoltaic and TEG system was examined by Bjork et al. [14] using an analytical model for four different types of commercial photovoltaic panels and a commercial Bi_2Te_3 TEG. The degradation of photovoltaic performance is occurred with temperature due to the TEG shown to be much faster than the increase in power produced by the TEG. Muhammad Fairuz Remeli et al. [15] designed and fabricateda lab scale bench-top prototype of waste heat recovery and electricity conversion system. This bench top system consists of Bismuth Telluride (Bi2Te3) based TEG sandwiched between two heat pipes. The first heat pipe was connected to the hot side of the TEG and the second to the cold side of TEG. The waste heat was simulated by using a 2 kW electric heater for heating the air in the system. Experiments were conducted to evaluate the system performance in terms of the heat transfer rate, heat exchanger effectiveness, and maximum output power. It was found that the highest heat exchanger effectiveness of 41% was achieved when the airspeed was set at 1.1 m/s. The system could recover around 1079 W of heat and produce around 7 W of electric power. This equated to 0.7% of thermal-to-electric conversion efficiency. The theoretical predictions showed good agreement compared to the experimental results. Seepana PraveenKumar et al. [16] used a thermo-electric cooling mechanism to cool a PV panel under real weather conditions. Results from the experimental process shows a significant temperature reduction in the modified PV module (i.e., cooled panel), an average temperature of 33.37 °C was recorded for the cooled PV module against 45.60 °C. The reduction was 12.23 °C in the PV module temperature which resulted in an electrical efficiency enhancement of 5.07%. In another hand, this module enhances the economics side due to the high power it generated during the experimental period. Salvador et al. [17] used a thermoelectric generators (TEGs) on house roofs because there is an extreme concentration of heat present on the roofs. A few works were reported in the literature about the thermoelectric generators for both sides theoretical and experimental. Therefore, the purpose of this study is to modeling thermoelectric generators on house roofs using the matrix laboratory (MATLAB) platform. In addition, an actual prototype of thermoelectric generators (TEGs) panel was examined and the results compared with the results from simulation. This study focus on explore the panel's potential for covering diverse surfaces such as building walls.

2. Experimental setup and materials

This chapter presents the experimental and theoretical work and measuring devices. It explains the design, material selection, manufacturing, assembling processes, components, computer simulation, laboratory equipment and implementations of the (TEGs panel) according to the study requirements. In this project (TEGs panel), a new heat-gaining system has been designed by SolidWorks and implemented in true by using multi thermoelectric generator modules (9 pieces of semiconductors) connecting in parallel to convert heat energy into electrical energy. All the results were obtained by testing the system practically and theoretically and making comparisons and discussions between them. The theoretical results were obtained through simulations using MATLAB software and the practical results were obtained through setting up a laboratory system and connecting it with the TEGs panel for recording the obtained results directly into the computer's memory.

The temperatures around the TEGs panel (hot side temperature T1, outside temperature T2 and ambient temperature Ta) were used as basic inputs for all theoretical and practical tests. Moreover, this study aims to examine the possibilities of using)TEGs panel (in various applications during exposure to various climatic conditions. As example, the TEGs panel is installing in the buildings for insulation and power generation or in remote areas. Finally, compare and discuss the results and find the gap between the theoretical and practical results for future works.

2.1. Thermoelectric (TEM)

TE converts either electricity to heat or heat to electricity. When the TE is used for cooling, referred to as (TEC), cooler modules are used electricity [18]. When the TE is used to generate electricity, it is also referred to as TEG. Semiconductors are mostly deposited in the form of free holes they are called type "P", and when most of them contain free electrons, it is known as type "N". The semiconductor materials used in electronic devices are precipitated under precise temperature and pressure conditions to control their concentration and distribution areas of points p and n. As semiconductor crystals can contain many p and n regions, p-n intersections between these regions are responsible for beneficial electronic behaviour. This behaviour involves determining the direction of electric current and converting heat energy to electrical energy; it has two sides, where heat or cold is shed on one side of the TEGs panel while the other side remains without any thermal effect. The purpose is to increase the amount of electrical energy produced on the panel electrodes due to the temperature difference on both sides of the panel.

2.1.1. Power of TEGs panel

The power and current provided by the TEG power can be easily calculated. The voltmeter should measure the volt (V) directly, while the ammeter should measure the current (I). Equation below determines the output power (P) from the generator in watts.

$$P = I \times V \tag{1}$$

The total heat input to the couple (Q_h) is:

$$Q_h = \left[\propto I\, T_h - \frac{1}{2} I^2 R - K(T_h - T_c) \right] \tag{2}$$

When: T_h is the temperature of the hot side of TEG, and T_c represent the temperature of the cold side of TEG. Seebeck coefficient (α), thermal conductivity (K) and electric resistance (R).

The following equations were used to calculate the seebeck coefficient (α), thermal conductivity (K) and electric resistance (R) [20].

$$\alpha = \frac{Q_{max}(T_h - \Delta T_{max})}{N T_h^2 I_{max}} \tag{3}$$

$$K = \frac{Q_{max}\,(T_h - \Delta T_{max})^2}{T_h^2\,\Delta T_{max}} \tag{4}$$

Table 1 lists the manufacturer's technical specifications of each TEG type used in this study. Besides, *R* is given for each TEG model.

TEG1 modules, primarily composed of N-type and P-type bismuth telluride (Bi2Te3) materials, find widespread application in power generation and temperature stabilization. These Thermoelectric Generators (TEGs) are easily accessible in the market at affordable prices, ensuring convenient installation and demonstrating notable longevity [25]. The N-type Bi3Te2 variant is notably suitable for thermoelectric generator applications, whereas the P-type Bi3Te2 variant is better suited for deployment in thermoelectric cooling systems [26].

The effective thermoelectric properties of the TEGs, such as coefficient (α), thermal conductivity (κ), and electric resistance (ρ) by using Equations (5)–(7) in this study and the manufacturer's technical specifications of the TEGs are summarized in Table 1 [21].

$$\alpha = \frac{Q_{max}(T_h - \Delta T_{max})}{N T_h^2 I_{max}} \tag{5}$$

$$\rho = \frac{A_{TEM} f (T_h - \Delta T_{max})^2}{2T_h^2 l}\;\frac{Q_{max}}{N^2 I_{max}^2} \tag{6}$$

$$\kappa = \frac{l_{TEM}(T_h - \Delta T_{max})^2}{A_{TEM} f T_h^2}\;\frac{Q_{max}}{\Delta T_{max}} \tag{7}$$

The properties of the lumped TE, such as S, R, and thermal conductance (K), are calculated based on the effective thermoelectric properties and technical specifications by using Equations (8)–(10). The lumped TE properties are used to determine the power output of the TEG (Fig. 1).

$$\mathrm{S} = 2\mathrm{N}\alpha \tag{8}$$

$$\mathrm{R} = \frac{4N^2 l\rho}{A_{TEM} f_p} \tag{9}$$

$$\mathrm{K} = \kappa \frac{A_{TEM} f_p}{l} \tag{10}$$

with no load (RL not connected), the open-circuit voltage as measured between points a and b expressed by Equation (11):

$$\mathrm{V} = \mathrm{S} \times \Delta\mathrm{T} \tag{11}$$

V is the output voltage from the couple (generator) in volts,

$$\Delta\mathrm{T} = T_h - T_c \tag{12}$$

T_h = temperature of the hot side of TEG,
T_c = temperature of the cold side of TEG.

Table 1
Technical specifications of the TEGs [22–24].

Technical Specification	TEG1-12,703	TEG1-12704	TEG1-12705	TEG1-12,706	TEG1-12,707	TEG1-12708	TEG1-12709	TEG1-12712	TEG1-12715
Material	Bismuth Telluride (Bi2Te3)								
Cover Surface	Ceramic plate: 96%Al2 O3, white (standard)								
N (number of thermo-element couples)	127								
Dimensions	40 × 40 × 3.9 mm								
ΔTmax (°C)	~70 °C								
Operating range	−40 °C (233.15 K) to 180 °C (453.15 K)								
(α)Thermo-electromotive force rate (μV/K)	185~220 μV/K								
(ð)Electrical conductivity (S/m)	800~1200 1/ohm.cm								
(K)Thermal Conductivity (W/m-K)	0.018–0.020W/K.CM								
(Z) Coefficient of merit	0.002695–0.003 K-1								
I max A	3	4	5	6	7	8	9	12	15
U max V	15.4								
(ρ)Electrical resistance Ω	3.42	3.02	2.51	1.98	1.71	1.51	1.36	0.91	0.75
Qcmax (w) ΔT = 0	26.7	36.8	46.5	53.3	62.2	71	80.1	106.7	133.3

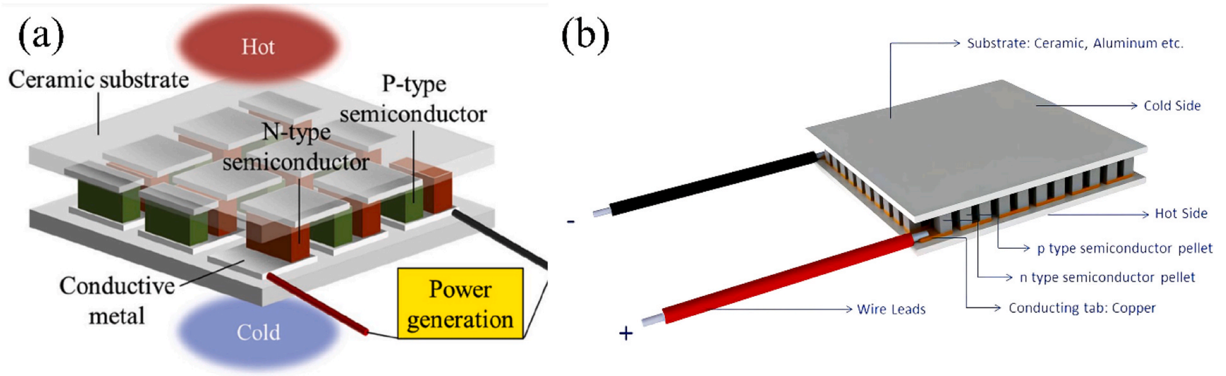

Fig. 1. Schematic of a thermoelectric energy generator TEG. (a) Effect of Heat on TEG Phases and determine the Power Generation using Lumped TEM. (b) Components of the Thermoelectric Generation Unit [27].

When a load is connected to the thermoelectric couple, the output voltage (V) decreased because of internal generator resistance. The Electrical current I is determined by Equation (13):

$$I = \frac{S \times \Delta T}{R_L + R_c} \tag{13}$$

(I) is the generator output current in amperes, R_L is the load resistance in ohms, R_c is the average internal resistance of TEG panel, The total heat input to the couple (Q_h) is:

$$Q_h = (S \times T_h \times I) - \left(0.5 \times I^2 \times R_c\right) + (K_c \times \Delta T) \tag{14}$$

K_c: is the lattice thermal conductivity

Another way to calculate the output power of the TEG is commonly measured by the maximum power point tracking method as reported in the previous study [19]. A simple numerical model was proposed by Paraskevas and Koutroulis [20] to predict the power output of the TEG. They have indicated that the maximum power transfer from the TEG source to the load was determined by the temperature difference of the TEG (ΔT), lumped seebeck coefficient (S), and a sum of the internal electric resistance (R). The power output model is expressed by Equation (6), which has complied with the TEG's actual power output.

$$P_{TEG} = \frac{S^2 \Delta T^2}{4 R_{TEG}} \tag{15}$$

2.1.2. Efficiency of TEG

The significance of the use of TEGs panel in the present study is to directly convert the heat flux into electrical energy through a phenomenon called a “Seebeck effect”.

The efficiency (η_g) of the thermoelectric generator can be calculated using the following expression 16:

$$\eta_g = \frac{P_O}{Q_h} x\ 100\% \tag{16}$$

The efficiency of a TEGs panel is the ratio of the electrical power output of the panel to the heat input to the panel. The heat input is the difference in temperature between the hot side and the cold side of the panel. The figure of merit (ZT) is a measure of the efficiency of a thermoelectric material. A higher ZT value means that the material is more efficient at converting heat into electricity [28].:

$$\eta_{\text{TEG}} = \frac{Po}{Qh} = \frac{\Delta T}{T_h} \times \frac{\sqrt{1 + ZT} - 1}{\sqrt{1 + ZT} + \frac{T_C}{T_h}} \tag{17}$$

where: (ΔT) the temperature difference between the hot side and the cold side of the panel, (ZT) the figure of merit of the thermoelectric materials used in the TEGs panel, T_h is the temperature of the hot side of TEG and T_c is the temperature of the cold side of TEG, (Q_h) the total heat input, and *Po* the power output of the panel.

The efficiency formula of a TEGs panel allows for the computation of its theoretical maximum efficiency. Nevertheless, the realized efficiency of a TEG panel will inevitably fall below this theoretical value due to several factors, including heat losses and electrical resistance. In this study, these deviations are addressed by applying correction ratios to mitigate these errors.

The figure of merit (ZT) functions as a quantitative metric for assessing the efficiency of thermoelectric materials. A heightened ZT value signifies an enhanced capacity for converting heat into electricity. The evaluation of material performance is predicated on the thermoelectric figure of merit, designated as Z and expressed in units of inverse Kelvin (1/K). This parameter establishes the material's efficiency in the context of transforming heat into electricity, specifically under a temperature gradient of 1 K (K).

$$\mathrm{ZT} = \frac{\alpha^2 \sigma}{k} T \tag{18}$$

where, σ is the electrical conductivity, κ is the thermal conductivity and T the temperature in Kelvin.

ZT = Z$\overline{\mathrm{T}}$ when the T is the average temperature in Kelvin

$$\overline{\mathrm{T}} = \frac{(T_h + T_c)}{2} \tag{19}$$

To compute the figure of merit (Z$\overline{\mathrm{T}}$) for the nine TEGs models connected in parallel under condition of sun and ice test conditions, the following procedural can be pursued.

1 Calculate the total electrical resistance (R total) of the TEGs in parallel.

$$R\mathrm{total} = \frac{1}{\frac{1}{R1} + \frac{1}{R2} + \ldots + \frac{1}{R9}} \tag{20}$$

where: R1, R2, …, R9 are the electrical resistances of TEGs in K/W12703, 12,704, 12,705, 12,706, 12,707, 12,708, 12,709, 12,712, and 12,715, respectively.

2 Calculate the total electrical conductivity (σ_total) of the TEGs in parallel.

$$\sigma\_\mathrm{total} = \frac{L}{R\_\mathrm{total}} \tag{21}$$

where: L is the thickness of the material in meters = 0.039 m [29].

3 Calculate the total Seebeck coefficient (α_total) of the TEGs in parallel.

$$\alpha\_total = \frac{\alpha 1 \ * \ A1 + \alpha 2 \ * \ A2 + \ldots + \alpha 9 \ * \ A9}{A1 + A2 + \ldots + A9} \tag{22}$$

where α1, α2, …, α9 are the Seebeck coefficients of TEGs, and A1, A2, …, A9 are their cross-sectional areas = 0.0016 m.

4 Calculating the total thermal conductivity (k_total) of the TEGs in parallel

$$k_{total} = \frac{1}{\frac{1}{K1} + \frac{1}{K2} + \ldots + \frac{1}{K9}} \tag{23}$$

where: K1, K2, …, K9 are thermal conductivity of TEGs.

5 Calculate the figure of merit (Z$\overline{\mathrm{T}}$_total) for the TEGs in parallel.

$$\mathrm{Z\overline{T}\_total} = \frac{\alpha\_total^2 \sigma\_total}{k\_total} \overline{\mathrm{T}} \tag{24}$$

$$\mathrm{Or\ Z\overline{T}\_total} = \frac{\mathrm{Z1} + \mathrm{Z2} + \ldots + \mathrm{Z9}}{9} \overline{\mathrm{T}} \tag{25}$$

where: Z1, Z2, …, Z9 are the figure of merit of the 9 TEGs connected in parallel.

This formula can be used to get a rough estimate of the efficiency of a TEGs panel.

The temperature difference across the hot and cold sides of a thermoelectric generator (TEG) directly influences the ZT value of the TEG panel. Consequently, the total ZT value (Z$\overline{\mathrm{T}}$_total) will be considered for both the sun test and the ice test scenarios.

To convert the temperatures from Celsius to Kelvin:

$$\text{Temperature in Kelvin (K)=Temperature in Celsius (°C)+273.15} \tag{26}$$

In the sun test, the TEGs panel displayed a temperature, with the highest reaching 68.7 °C and the lowest at 32 °C. The respective average temperatures, T_hot avg and T_cold avg, were computed as 58.8 °C and 57.3 °C [4]. Consequently, this analysis yielded an approximate cumulative figure of merit (Z$\overline{\mathrm{T}}$_total (avg)) of 0.07549 for the TEG panel under sun test conditions. During the ice test, the average temperatures shifted, with T_hot avg and T_cold avg recorded as 9.7 °C and 1.5 °C, respectively. This evaluation led to an approximate Z$\overline{\mathrm{T}}$_total value 0.18406 of for the TEG panel in the context of ice test conditions. This is a relatively low Z$\overline{\mathrm{T}}$, but it is still good enough for some thermoelectric applications, such as generating electricity from weather or waste heat. Since a complete module consists of several couples, therefore it is necessary to rewrite our equation for an actual module, as explained in Equations (27) and (28).

$$Vo = SM\ x \Delta T = I\ x\ (RM + RL) \tag{27}$$

Vo is the output of the generator in volts, *SM* is the module's average Seebeck coefficient in volts/°K, *RM* is the module's moderate resistance in ohms.

$$I = \frac{Ns \times SM \times \Delta T}{\frac{Ns \times RM}{Np} + RL} \tag{28}$$

Ns number of modules connected in series, *Np* number of modules connected in parallel

The Output Power (P_O) from the generator in watts is determined by Equation (19).

$$P_O = Vo \times I \tag{29}$$

The operational efficiency of the TEG panel is notably contingent upon the alterations in temperature between its hot and cold sides within the sun and ice tests. Consequently, these temperature variations directly influence the power outputs of the TEG panel, consequently affecting its overall efficiency. To ascertain the TEG panel's efficiency over time, the following Equation (30) can be employed: [4].

$$\eta_{TEGs\ panel} = \frac{Po}{Qh} = \frac{\Delta T}{T_h} \times \frac{\sqrt{1 + Z\overline{T}} - 1}{\sqrt{1 + Z\overline{T}} + \frac{T_C}{T_h}} \tag{30}$$

The module efficiency is an important factor especially when the available heat is limited, the maximum efficiency conversion is given by Equation (31).

$$\eta\_max = \frac{P_{max}}{\dot{Q}_{hot}} \tag{31}$$

where, $\dot{Q}_{hot}$ is the heat that flows on the hot surface of cell and P_{max} is maximum power.

Through MATLAB calculations and experimental data, the efficiency profile ($\eta_{TEGs\ panel}$) over time can be elucidated. Importantly, it should be acknowledged that the effective $Z\overline{T}$ value of the nine parallelly connected TEGs may experience a slight reduction relative to the calculated value. This decline is attributed to loss within the interconnections among the TEGs units.

2.1.3. *Diff* correction ratio

The ***Diff*** equation is utilised to calculate the variance ratio and to calculate the difference or discrepancy between the MATLAB simulation results (Mat), and the experimental results (Exp) expressed as a percentage. The resulting value represents the percentage difference between the MATLAB simulation and the experimental results. It helps quantify the level of agreement or discrepancy between the two datasets. A value of 0% would indicate perfect agreement, while a non-zero value would indicate a difference between

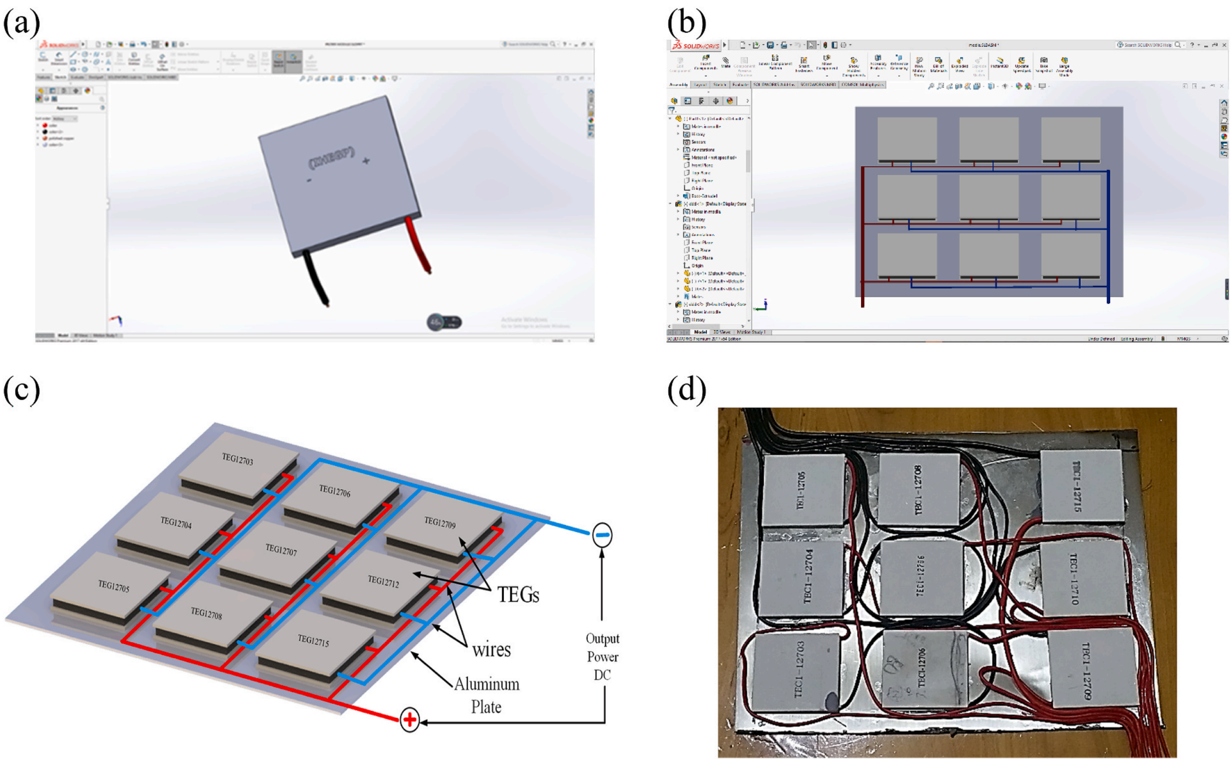

Fig. 2. Modeling and Assembling of (TEGs panel) by SOLIDWORKS. (a) Modelling one unit of TEG by Solidworks. (b) Modelling and connecting nine units of TEGs by Solidworks. (c) Schematic Diagram of Assembling TEGs panel by Solidworks. (d) Implementation of the TEGs Panel in Reality.

the two sets of results.

$$Diff = \left[\frac{Mat - Exp}{Exp}\right] \times 100\% \tag{32}$$

$$Diff \text{ correction ratio} = \frac{Avr1 + Avr2}{2}\%.. \tag{33}$$

when Avr 1 is the Average Diff of the first test, and Avr 2 is the Average Diff of the second test.

$$Avr = \frac{\text{Maximum}Diff + Minmum\ Diff}{2}\% \tag{34}$$

2.2. Modelling and design of TEGs panel

A simple design was built initially, and it is preliminary project imagery to implement the idea. To design the system, SOLIDWORKS was used to draw and design the panel. Also, the primary generation unit was designed by SOLIDWORKS after taking the realistic dimensions as shown in Fig. 2. In addition to the design of the heat-absorbing sheet cover (Aluminum sheet), The rectangular cover shown in Fig. (3) is made of aluminium. (20 × 16) cm and (1 mm) thickness can easily carry the system's weight and stabilise it.

2.3. Materials

Two main types of sorbents and heat transfer materials used in this study with different specifications and places. Aluminium exterior covers facing the direct thermal effect and are used to absorb heat from the outside, distribute them over a larger area, and then transfer them to the inside Surface temperature of the absorber plate (aluminium sheet 6061). The thermal properties of an aluminium sheet with a thickness of 1 mm can vary depending on the specific alloy and temper of the material. A general-purpose aluminium alloy (e.g. 6061) used in this study, the thermal conductivity: is 151–202 W/mK, approximately 167 W/mK at room temperature, and the Specific heat capacity is 0.9 J/gK, Density is 2.7 g/cm^3 [30]. These values can be used to calculate the heat transfer characteristics of an aluminium sheet with a thickness of 1 mm in a TEGs panel.

2.4. Assembling TEGs panel

The primary method of operation in this study depends mainly on the generated electricity directly by semiconductors through the difference in temperature (ΔT) between the two sides of the panel. Aluminium sheets distribute the thermal energy generated on both sides of the TEGs panel to the area of the panel as shown in Fig. 4. At the same time, aluminium sheets collect and absorb the heat energy from both sides and are then transported inward to the ceramic cover of the main generating units of TEGs through a thermal adhesive. Each generating unit of TEG consists of 127 semiconductor elements as shown in Fig. 1. Each point absorbs thermal energy and directly turns it into simple electrical power by releasing electrons. This electrical power is generated at the points collected by precise electrical connections, which are interconnected and placed within the panel. The power is collected from all the points inside the TEGs panel on its poles and transmitted through copper wires. All nine main units of TEGs are connected in parallel. The polarity of the panel (+ or -) depends on the direction of the electron's movement, which in turn depends on the conditions surrounding the TEGs panel as presented in Fig. 1. Nine TEGs generating units were selected to make the project's zero models with different generating capacities (Fig. 3).

2.5. MATLAB simulation

A mathematical simulation was used to know the potential of this panel when used in various power generation applications and

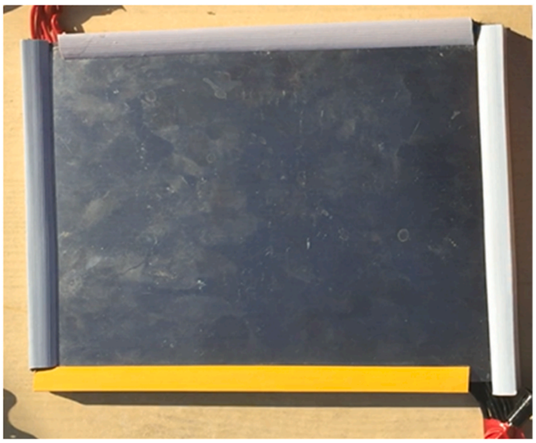

Fig. 3. The prototype of TEGs panel.

Fig. 4. Measurement devices and functional test setup for TEGs panel for (a) DT-3891G Multi-Digital Thermometer Data Logger for temperature measurement, (b) Fluke VT04 Visual Infrared Thermometer for monitoring temperatures and heat transfer during the tests, (c) VICTOR 86E AC-DC Multi-Function Meter for measuring the current and voltage output power from the TEGs panel, (d) Schematic diagram illustrating the operating test system and (e) exposing TEGs panel to the ice cubices and sunlight.

comparing the results from Matlab with experimental results. All variables and unique inputs for each generating unit (TEGs) were considered in this study. In addition, all data were simulated together through mathematical calculations to obtain the most accurate results and compare them with experiments. The temperatures around the board (Hot side temperature T1, outside temperature T2 and ambient temperature Ta) were taken from a multi-digital thermometer data logger. All the factors can be affecting the power output of each TEG generation unit in the panel were taken into consideration, such as coefficient (α), thermal conductivity (κ), and electric resistance (ρ) these variables are different of each TEG unit. The efficiency was calculated according to the total power generated and total heat input. The experimental setup for tools and equipment used in this study are shown in Fig. 4. A thermal IR camera and digital thermocouple were used during the test. TEGs panel was exposed to the hot source and then to the cold source.

2.6. Error analysis

In this section, the errors in different instruments can be occurred due to measuring or using. To estimating the possible error in calculation, Seepana PraveenKumar [31] used a method to calculate the uncertainty that allied with instruments and calculations of

Table 2
Accuracy of the experimental measurements of the equipment used in this study [31].

No	Equipment measurements	Range	Units	Basic Accuracy %
1	DT-3891G Multi-Digital Thermometer Data Logger for temperature [32].	−200 °C to +1372 °C Type K	°C	±[0.15%rdg+1 °C]
2	Fluke VT04 Visual Infrared Thermometer for monitoring temperatures and heat transfer during the tests [33].	−10 °C to +250 °C	°C	±2 °C or ±2% of reading in °C, whichever is the greater (at 25 °C nominal)
3	VICTOR 86E AC-DC Multi-Function Meter for current and voltage output power from the TEGs panel [34].	220 mV to 220 V	V	±(0.05%+8d) in DC
		2000μA/20 mA	A	±(0.5%+4d) in DC
		200 mA		±(0.8%+6d) in DC
		10 A		±(2.0% + 15d) in DC

the experimental results. The accuracy of the instrument and the minimum values of the output were used to calculate the errors as listed in Table 2.

3. Results and discussion

The experimental results of the generating electric power possibility when the panel is placed outside and exposed to the sun or ice are shown in Fig. 6. (a–d), while the other side of the panel is under the shadow (no affections). It was noticed that the rapid response of TEGs panel is occurred when exposed directly to heat sources such as hot weather or cold sources.

Fig. 6 (a and b) shows the temperature difference observed on both sides of the TEGs panel during the sun and ice experiments. In the sun test Fig. 6-a, (T2) represents the temperature of the hot side of the TEGs panel, which is directly exposed to the sun's rays. While (T1) represents the temperature of the cold side, which is in the shadow and exposed to the ambient temperature. During the ice test Fig. 6-b, (T2) still denotes the temperature of the hot side, but in this case, it is shielded from the sun and exposed to the ambient temperature, (T1) represents the temperature of the cold side of the TEGs panel when it is exposed to the cubic ice. The experimental tests commence with the TEGs panel's both sides at an initial temperature of 32 °C. This step ensures that any variations in thermal and electrical behaviors are primarily influenced by temperature differences over time. In contrast, the ambient temperature remains relatively constant throughout the test duration, also at 32 °C.

Fig. 6-a shows The maximum $\triangle$T was (3.3°) when (T2) was (43.1°), and (T1) was (39.8°), Note that (T2) is increasing rapidly due to exposure to sunlight directly, while (T1) increases relatively less due to the temperature affected by ambient temperature (under the shadow). Fig. 6-b shows the maximum $\triangle$T was (18°) when (T2) was (21.7°), and (T1) was (3.7°) during ice test, Note that (T1) is decreasing rapidly due to exposure to cubic ice directly, while (T2) decreasing relatively less due to the temperature affected by ambient temperature (under the shadow).

Fig. 6 (c and d) show It is observed that any simple increase in difference in temperature (ΔT) corresponds to an increase in energy produced (W), where (T2) and (T1) is the temperatures of the hot and cold faces of TEG panel [35]. After a period time and due to the air temperature exceeding 32°, both sides of the panel converge, resulting in a decrease in the energy generated because of reducing ΔT. Fig. 6-c shows that the highest value for ΔT during the sun test was 3.3° in the 12th minute, leading to obtaining the highest power generated value by 0.429 W in the 14th minute. In addition, Fig. 6-d shows the highest value for ΔT during cubic ice test was 18° in the 10th minute, which result in obtaining the highest power generated value by 8.04437 W in the 11th minute. The observed delay in power generation can be attributed to the thermal distribution and absorption processes occurring within the panel material layers, specifically between the aluminium sheet and the TEGs units [36]. As a result, the temperature difference increases, leading to a subsequent increase in energy generation with a delay of one or 2 min. Fig. 5 visually illustrates the heat transfer processes within the TEGs panel, providing a better understanding of the time dynamics observed during experimental.

Fig. 7 (a) and (b) provide a visual representation of the comparison between the power generation obtained by MATLAB simulation and experimental results. The power experiment results (P_exp) are based on the direct measurements of voltage and current obtained from the measuring devices during the tests. In contrast, the power Matlab results (P_mat) are derived from calculated voltage and current values, which it influenced by various factors. These factors include the input parameters, system characteristics, and mathematical models employed in the MATLAB program. Therefore, the generated energy diagram in the MATLAB program represents an estimation based on the simulated values rather than direct measurements. Fig. 8 (a) and (b) show the differences between the efficiency from experimental work (η_exp) and MATLAB simulation (η_mat) during the sun and ice tests. The obtained results of efficiency (η) for the TEGs panel were generally good. However, these results provide a starting point for future enhancements and optimisations to enhance the efficiency of the TEGs panel. The efficiency of the TEGs panel is determined based on Equation (30). The

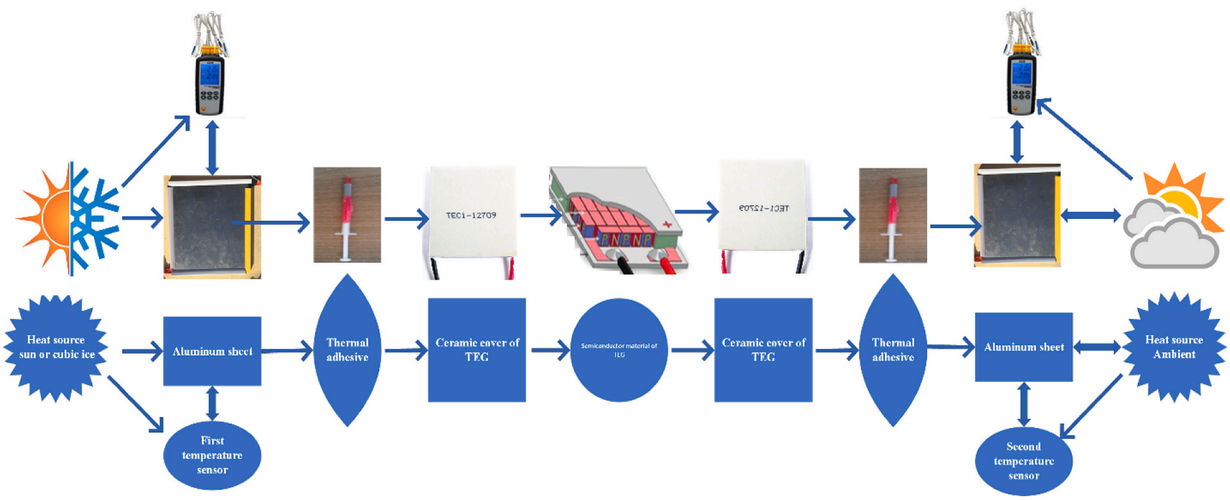

Fig. 5. Schematic diagram of heat transfer processes in the TEGs panel and illustrating the delay in response.

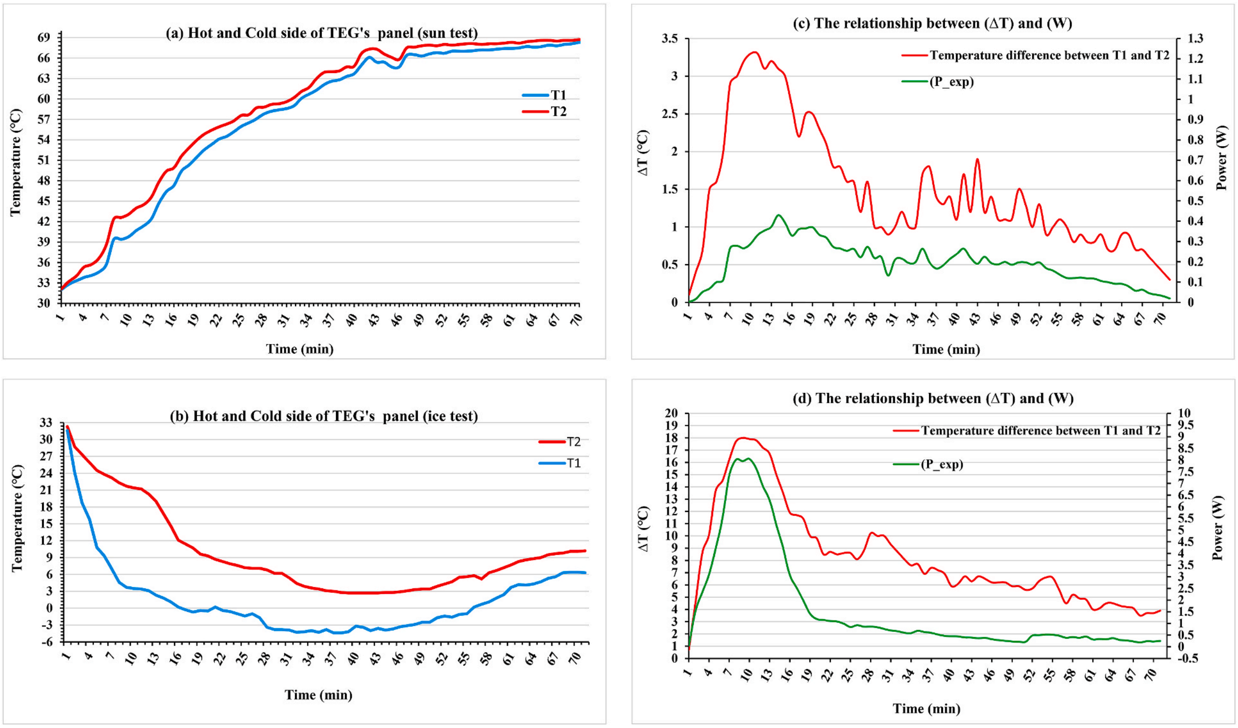

Fig. 6. Experimental result of TEGs panel. (a) Temperature variation (T1 and T2) on both sides of the TEG panel during sun test and (b) during the ice test. (c) The energy generated (W) and temperature difference (ΔT) during sun test and (d) during the ice test.

maximum and minimum efficiency recorded in both tests are shown in Table 4.

According to the results shown in Figs. 6–8, it can be noticed that the results generated by the MATLAB program closely match the experimental results. The discrepancy in the results obtained can be attributed to two reasons which are power losses occurring during the energy transfer process between the conductors within the TEGs panel. Furthermore, these losses can occur from various sources such as resistance, impedance, or inefficiencies in the electrical components leading to a difference between the simulated and actual curves. Another reason is latent heat within the system contributes to the observed variance. Latent heat refers to the energy absorbed or released during the TEGs panel working or heat absorbed and heat released during a phase change, such as converting a solid to a liquid in cubic ice test [37]. In addition, this latent heat can affect the overall energy dynamics within the TEGs panel [38], which leads to deviations between the simulated and experimental power generation results. This disparity arises from the inherent difficulty that faces Matlab calculations in accurately capturing the time response of heat transfer. Calculating the response time of heat transfer for the TEGs panel becomes significantly challenging due to the intricate nature of heat transfer across multiple layers within the TEGs panel. This discrepancy gives us a better understanding of the observed variations between the MATLAB simulation and the experimental results. Furthermore, this understanding allows us to focus on improving the accuracy of simulations by addressing these discrepancies leading to further validating the reliability of the MATLAB simulation outcomes. Table 3 and Table 4 list valuable tools for finding the Diff ratio to obtain accurate predictions of efficiency and power generation dynamics in the TEGs panel. The Diff ratio equation effectively corrects and adjusts the simulation results obtained from the MATLAB program. The accuracy and reliability of the simulation outcomes can be improved by using this equation, thereby achieving a more precise representation of the efficiency and power processes within the TEGs panel.

During the sun exposure test, as shown in Fig. 6 (a), the delay response ranges from 1 to 3 min. However, in the ice exposure test, as depicted in Fig. 6 (b), the delay time increases from 3 to 6 min. This delay can be attributed due to the to the rapid melting of ice on the first face of the TEGs panel. As a result, latent heat is released during the phase change, where the ice transforms from a solid to a liquid state. This process affects the thermal distribution and absorption within the panel [39], leading to a noticeable delay in the response time. Fig. 9 (a and b) illustrates the anticipated outcomes when using the Diff ratio to calculate the discrepancies. The power generation curves generated by the MATLAB program are expected to approximately match with the experimental results. It was postulated that the temperature difference increases at a rate of 1 °C per minute until reaching 70 °C. The results indicate that the maximum electric power of 57.44 W can be achieved when ΔT is 70 °C, with maximum efficiency (η) of 13.5%.

4. Conclusions and recommendations

In this study, the experiments tests revealed that the proposed power generation for single plate could generate average electric powers by 8.04 W and 0.4029 W when exposed to ice and sun, respectively. It was found that the efficiency reached to 16.243% in the

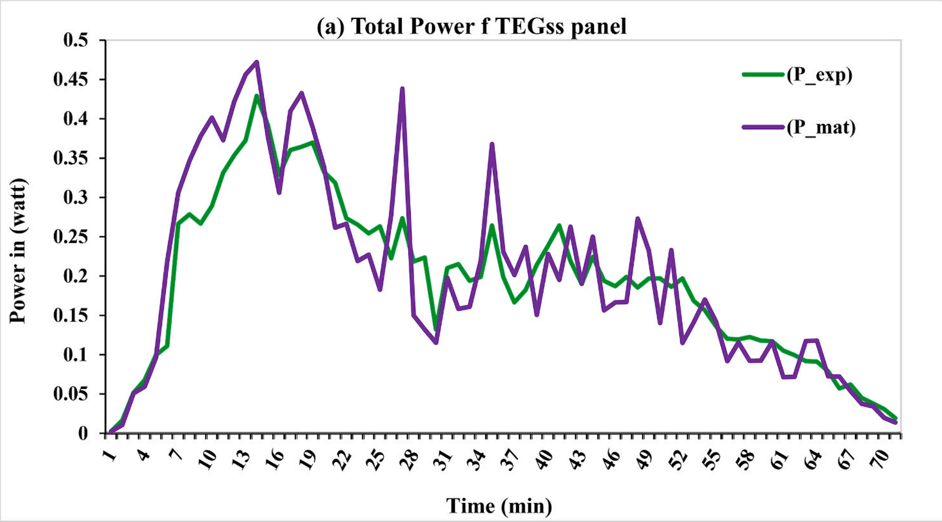

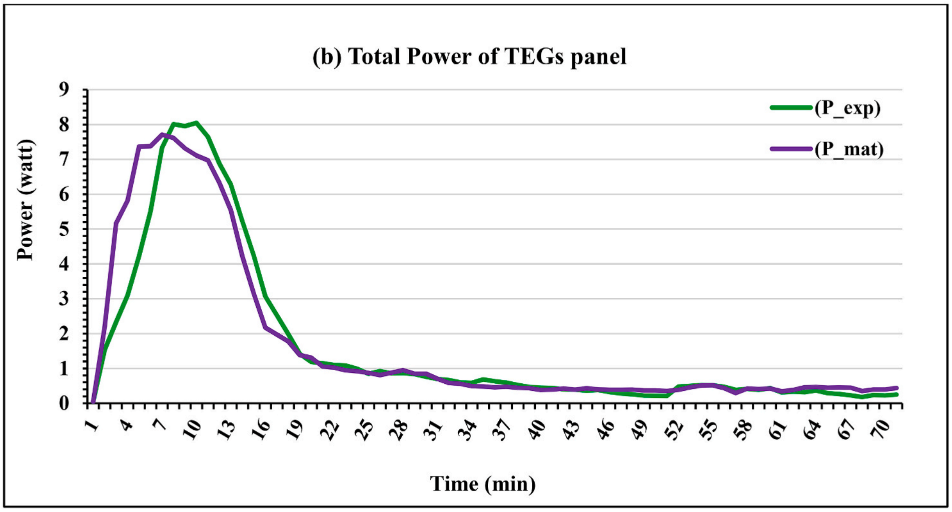

Fig. 7. Matlab and experimental result of TEGs power generating during the time for (a) sun test and (b) ice test.

ice test and 10.277% in the sun test. The results showed that the diff correction ratio was 6.5975% for power trends validation and 5.46% for efficiency trends validation according to the results of experiments and Matlab. It is concluded that the TEGs panel was acceptable to use as an economically system with acceptable efficiency and environmental sustainability. Furthermore, The TEGs panel can be operating within temperatures ranges from −20 °C to 80 °C, making it suitable for day and night usage. The results indicated that the several energy-harvesting blocks are connected in series or parallel which can collectively serve as an independent and semi-permanent power source. This configuration allows that the total energy production and efficiency can be increased by augmenting several factors simultaneously. It was found that utilising advanced materials and technologies enhances the energy-harvesting capabilities of the TEGs panel and increase their power output. It was observed that the TEGs panels have advantage by using thermal energy instead of using sunlight only in comparison with solar photovoltaics. Besides, this allows for continuous electricity generation throughout all the time (day or night) as temperature difference (ΔT) does not equal zero or surpasses more than 72 °C.

The prototype of TEGs panel with small area is not exceeding 0.032 m^2 can generate a good amount of energy considering its size and cost, which in turn can be used to cover larger surfaces such as roofs and walls of buildings. Thus, the promising potential of TEGs panels is considered a major source of sustainable energy in the future leading to take a huge step forward in the field of renewable energy. This study recommended that the more experiments can be conducted by using batteries to store excess energy and then used when needed. In addition, benefit from practical solar system development to generate electricity and cooling. This study gives insight for promoting solar energy as a sustainable alternative to conventional sources.

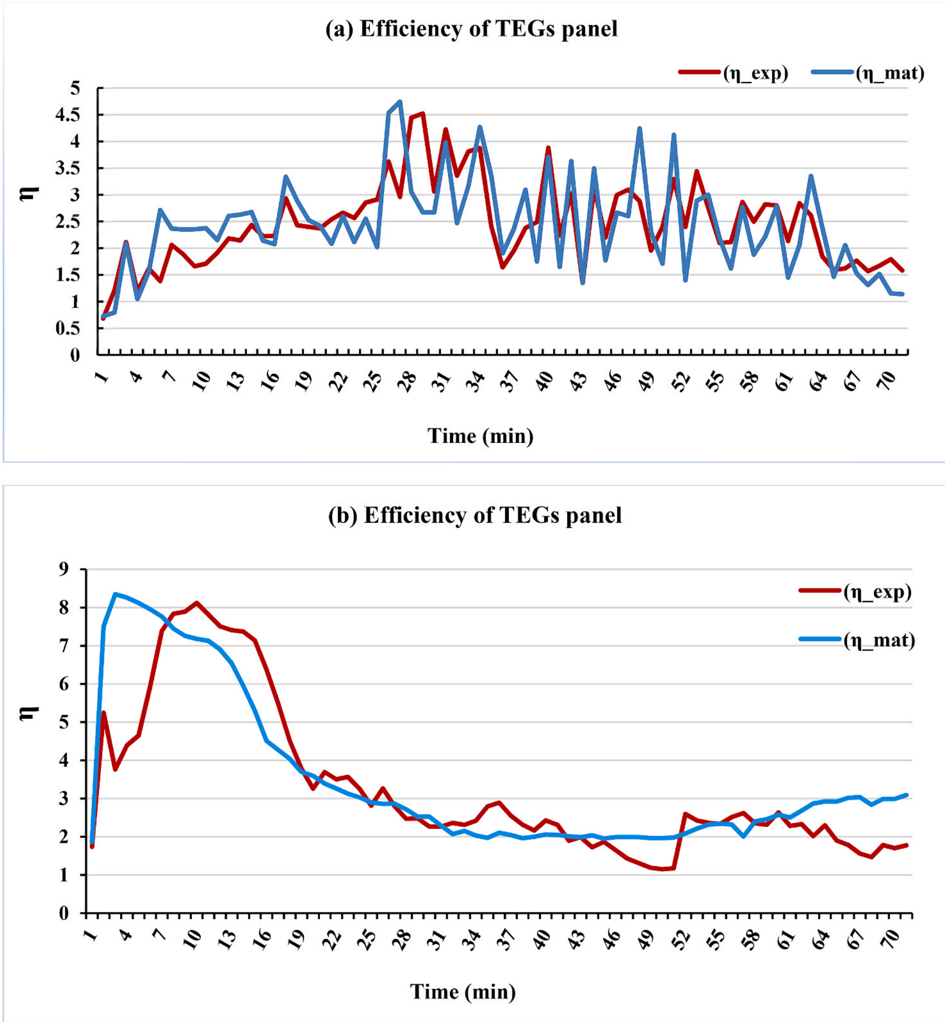

Fig. 8. Matlab and experimental result of TEGs efficiency during the time for (a) sun test and (b) ice test.

Table 3
Power correction ratio comparison between MATLAB simulation and experimental results.

Test type	Maximum (P_mat)	Maximum (P_exp)	Maximum Diff	Minimum (P_mat)	Minimum (P_exp)	Minimum Diff	Average Diff
Sun test	0.472	0.429	10.02%	0.0023	0.0022	4.54%	7.28%
Ice test	7.707	8.04	4.14%	0.049	0.0455	7.69%	5.915%
Diff correction ratio							6.5975%

Table 4
Efficiency correction ratio comparison between MATLAB simulation and experimental results.

Test type	Maximum (η_mat)	Maximum (η_exp)	Maximum Diff	Minimum (η_mat)	Minimum (η_exp)	Minimum Diff	Average Diff
Sun test	4.742	4.522	4.87%	0.723	0.68	6.2%	5.54%
Ice test	8.348	8.121	2.79%	1.869	1.735	7.96%	5.38%
Diff correction ratio							5.46%

CRediT authorship contribution statement

Hiba ali Hussein: Methodology, Software, Resources. **Zhonglai Wang:** Idea, Project administration, Supervision. **W.K. Alani:** Validation, Funding acquisition, Formal analysis, Results analysis. **J. Zheng:** Writing – original draft, Preparation, Writing – review & editing, Visualization. **M.A. Fayad:** Writing, and experimental setup, All authors have read and agreed to the published version of the

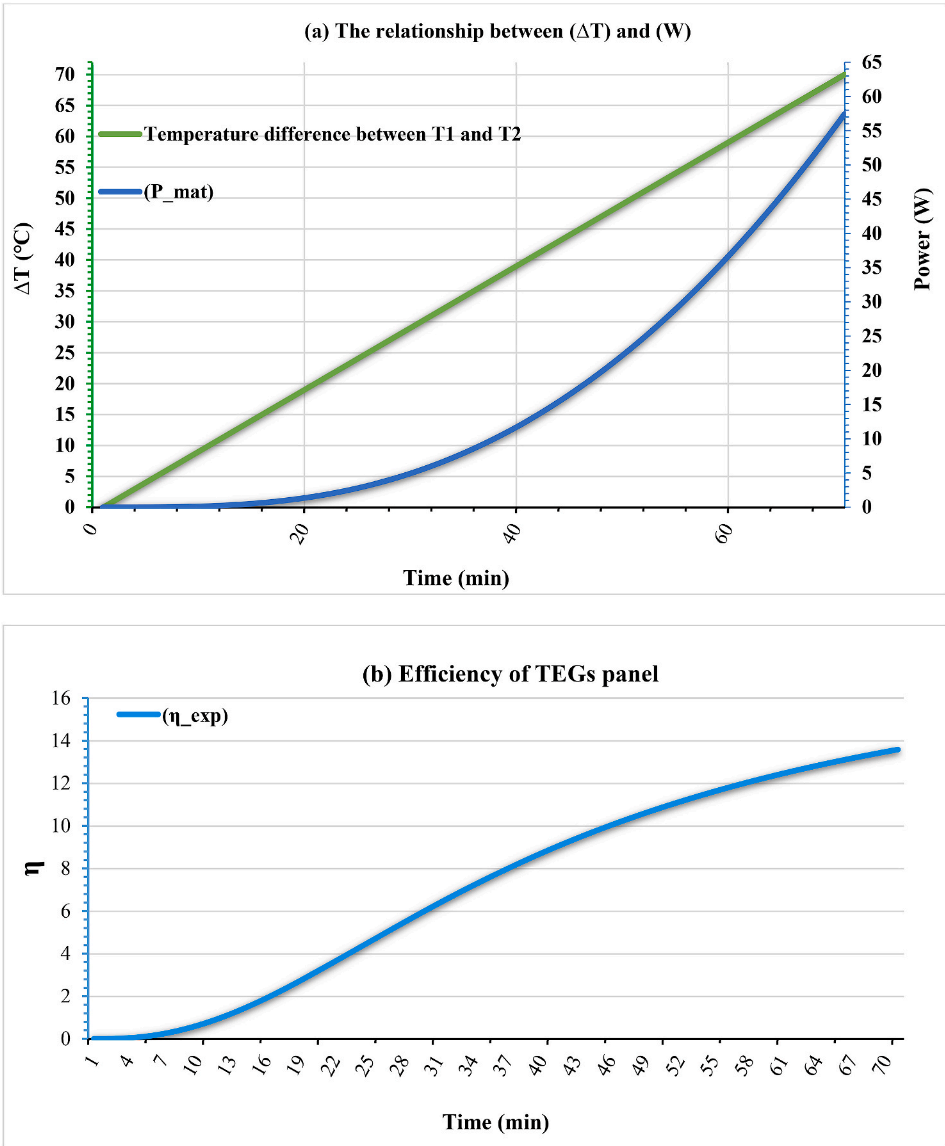

Fig. 9. Matlab simulation result of TEGs after using diff ratio: for (a) Power Generation (P_mat) as a Function of ΔT during the time and (b) for the corresponding efficiency during the time.

manuscript.

Declaration of competing interest

The authors confirm and declare that there is no conflict of interests regarding the publication of this paper.

Data availability

Data will be made available on request.

References

[1] D. Champier, Thermoelectric Generators: A Review of Applications, Energy Conversion and Management, 2017, https://doi.org/10.1016/j.enconman.2017.02.070.
[2] O. Ando Junior, N. Calderon, S. de Souza, Characterization of a thermoelectric generator (TEG) system for waste heat recovery, Energies 11 (6) (Jun. 2018) 1555, https://doi.org/10.3390/en11061555.
[3] X.F. Zheng, C.X. Liu, R. Boukhanouf, Y.Y. Yan, W.Z. Li, Experimental study of a domestic thermoelectric cogeneration system, Appl. Therm. Eng. 62 (1) (Jan. 2014) 69–79, https://doi.org/10.1016/j.applthermaleng.2013.09.008.

[4] S. Praveenkumar, E.B. Agyekum, A. Kumar, V.I. Velkin, Thermo-enviro-economic analysis of solar photovoltaic/thermal system incorporated with u-shaped grid copper pipe, thermal electric generators and nanofluids: an experimental investigation, J. Energy Storage 60 (January) (2023), 106611, https://doi.org/10.1016/j.est.2023.106611.

[5] M.A. Qasim, N.T. Alwan, S. PraveenKumar, V.I. Velkin, E.B. Agyekum, A new maximum power point tracking technique for thermoelectric generator modules, Inventions 6 (4) (Nov. 2021) 88, https://doi.org/10.3390/inventions6040088.

[6] X.F. Zheng, C.X. Liu, R. Boukhanouf, Y.Y. Yan, W.Z. Li, Experimental study of a domestic thermoelectric cogeneration system, Appl. Therm. Eng. (2014), https://doi.org/10.1016/j.applthermaleng.2013.09.008.

[7] D. Kraemer, et al., High-performance flat-panel solar thermoelectric generators with high thermal concentration, Nat. Mater. (2011), https://doi.org/10.1038/nmat3013.

[8] K. McEnaney, D. Kraemer, Z. Ren, G. Chen, Modeling of concentrating solar thermoelectric generators, J. Appl. Phys. (2011), https://doi.org/10.1063/1.3642988.

[9] C. Lertsatitthanakorn, N. Khasee, S. Atthajariyakul, S. Soponronnarit, A. Therdyothin, R.O. Suzuki, Performance analysis of a double-pass thermoelectric solar air collector, Sol. Energy Mater. Sol. Cells (2008), https://doi.org/10.1016/j.solmat.2008.03.018.

[10] W. He, Y. Su, S.B. Riffat, J.X. Hou, J. Ji, Parametrical analysis of the design and performance of a solar heat pipe thermoelectric generator unit, Appl. Energy (2011), https://doi.org/10.1016/j.apenergy.2011.07.017.

[11] W. He, Y. Su, Y.Q. Wang, S.B. Riffat, J. Ji, A study on incorporation of thermoelectric modules with evacuated-tube heat-pipe solar collectors, Renew. Energy (2012), https://doi.org/10.1016/j.renene.2011.06.002.

[12] E.A. Chávez-Urbiola, Y.V. Vorobiev, L.P. Bulat, Solar hybrid systems with thermoelectric generators, Sol. Energy (2012), https://doi.org/10.1016/j.solener.2011.10.020.

[13] E.A. Chávez Urbiola, Y. Vorobiev, Investigation of solar hybrid electric/thermal system with radiation concentrator and thermoelectric generator, Int. J. Photoenergy (2013), https://doi.org/10.1155/2013/704087.

[14] R. Bjørk, K.K. Nielsen, The performance of a combined solar photovoltaic (PV) and thermoelectric generator (TEG) system, Sol. Energy (2015), https://doi.org/10.1016/j.solener.2015.07.035.

[15] M.F. Remeli, et al., Experimental investigation of combined heat recovery and power generation using a heat pipe assisted thermoelectric generator system, Energy Convers. Manag. (2016), https://doi.org/10.1016/j.enconman.2015.12.032.

[16] S. Praveenkumar, E.B. Agyekum, N.T. Alwan, M.A. Qasim, V.I. Velkin, S.E. Shcheklein, Experimental assessment of thermoelectric cooling on the efficiency of PV module, Int. J. Renew. Energy Resour. 12 (3) (2022) 1670–1681, https://doi.org/10.20508/ijrer.v12i3.13087.g8553.

[17] C.S. Salvador, A. Caliwag, N. Zaldivar, V. Angeles, M. Bernabe, Modeling of roof-mountable thermoelectric generators, in: Proceedings - 25th International Conference on Systems Engineering, ICSEng 2017, 2017, https://doi.org/10.1109/ICSEng.2017.75.

[18] W.K. Alani, J. Zheng, M.A. Fayad, L. Lei, Enhancing the fuel saving and emissions reduction of light-duty vehicle by a new design of air conditioning worked by solar energy, Case Stud. Therm. Eng. (2022), https://doi.org/10.1016/j.csite.2022.101798.

[19] C. Yu, K.T. Chau, Thermoelectric automotive waste heat energy recovery using maximum power point tracking, Energy Convers. Manag. (2009), https://doi.org/10.1016/j.enconman.2009.02.015.

[20] A. Paraskevas, E. Koutroulis, A simple maximum power point tracker for thermoelectric generators, Energy Convers. Manag. (2016), https://doi.org/10.1016/j.enconman.2015.11.027.

[21] M. Chen, G.J. Snyder, Analytical and numerical parameter extraction for compact modeling of thermoelectric coolers, Int. J. Heat Mass Tran. (2013), https://doi.org/10.1016/j.ijheatmasstransfer.2013.01.020.

[22] Wellentech, [Interenet]. [Cited 3 August 2023], Vailable from URL: https://www.wellentech.cn/index.html.

[23] Thermoelectric-reference-guide, [Interenet]. [Cited 3 August 2023], Vailable from URL: https://thermal.ferrotec.com/technology/thermoelectric-reference-guide/thermalRef13/.

[24] Thermoelectric-peltier-cooler, [Interenet]. [Cited 3 August 2023], Vailable from URL: https://rees52.com/tec1-12706-thermoelectric-peltier-cooler-12-volt-92-watts-ab038-460-temprature-and-humidity-sensors/?search_query=TEC&results=292.

[25] T. Lu, et al., Synergistically enhanced thermoelectric and mechanical performance of Bi2Te3 via industrial scalable hot extrusion method for cooling and power generation applications, Mater. Today Phys. 32 (Mar. 2023), 101035, https://doi.org/10.1016/j.mtphys.2023.101035.

[26] A. Nozariasbmarz, J.S. Krasinski, D. Vashaee, N-type bismuth telluride nanocomposite materials optimization for thermoelectric generators in wearable applications, Materials 12 (9) (May 2019) 1529, https://doi.org/10.3390/ma12091529.

[27] Y.-S. Byon, J.-W. Jeong, Phase change material-integrated thermoelectric energy harvesting block as an independent power source for sensors in buildings, Renew. Sustain. Energy Rev. 128 (Aug. 2020), 109921, https://doi.org/10.1016/j.rser.2020.109921.

[28] H. Jouhara, et al., Thermoelectric generator (TEG) technologies and applications, Int. J. Thermofluids 9 (Feb. 2021), 100063, https://doi.org/10.1016/j.ijft.2021.100063.

[29] S. Edition, Free convection 112 (2015), https://doi.org/10.1007/978-3-319-15793-1_19.

[30] M.C.H.M. Rao, "EXPERIMENTAL INVESTIGATION ON IMPROVEMENTS IN MECHANICAL PROPERTIES OF AA2024/AL203/B4C HYBRID COMPOSITE." Andhra University..

[31] S. PraveenKumar, E.B. Agyekum, A. Kumar, V.I. Velkin, Performance evaluation with low-cost aluminum reflectors and phase change material integrated to solar PV modules using natural air convection: an experimental investigation, Energy 266 (Mar. 2023), 126415, https://doi.org/10.1016/j.energy.2022.126415.

[32] Thermocouple-thermometers [Interenet]. [Cited 3 August 2023], Vailable from URL: https://emin.asia/cemdt-3891g-cem-dt-3891g-k-type-j-type-thermocouple-thermometers-type-k-j-four-inputs-68275/pr.html.

[33] Temperature-measurement, [Interenet]. [Cited 3 August 2023], Vailable from URL: https://www.fluke.com/en-us/product/temperature-measurement/ir-thermometers/vt04#.

[34] Digital-multimeter, [Interenet]. [Cited 3 August 2023], Vailable from URL: http://www.victor-multimeter.com/products/digital-multimeter/digital-multimeter/digital-multimeter-victor-86e-667.html.

[35] J.L. Zeng, X. Liu, C.Q. Su, Y.P. Wang, X. Xiong, Numerical investigation of a geothermal thermoelectric generator using gravity heat pipe structure, Energy Rep. 9 (2023) 1237–1246.

[36] X. Bao, S. Hou, Z. Wu, X. Wang, L. Yin, Y. Liu, H. He, S. Duan, B. Wang, J. Mao, F. Cao, Mechanical properties of thermoelectric generators, J. Mater. Sci. Technol. 148 (10) (2023).

[37] T. Li, Y. Fu, C. Dong, D. Li, H. Gu, Y. Ye, Factors influencing the thermoelectric characteristics of a thermoelectric generator with cold-side micro heat pipe arrays, J. Power Sources 557 (2023), 232493.

[38] M.W. Tian, I.B. Mansir, S.M. Eldin, H. Ayed, H. Loukil, N. Alkhamis, Economic and thermal performance analysis of two-stage thin-film solar thermoelectric power generator, Case Stud. Therm. Eng. 45 (2023), 103012.

[39] M. Ge, Z. Li, Y. Zhao, L. Xie, S. Wang, Effect of exhaust parameters on performance of intermediate fluid thermoelectric generator, Case Stud. Therm. Eng. 28 (2021), 101480.